



The Rieske iron-sulfur protein is a primary target of molecular hydrogen

Shuto Negishi ^{a,1}, Mikako Ito ^{a,1}, Tomoya Hasegawa ^a, Hikaru Otake ^a, Bisei Ohkawara ^a, Akio Masuda ^a, Hiroyuki Mino ^b, Tyler W. LeBaron ^{c,d,*}, Kinji Ohno ^{a,e,*,¹}

^a Division of Neurogenetics, Center for Neurological Diseases and Cancer, Nagoya University Graduate School of Medicine, Nagoya, 466-8550, Japan

^b Division of Material Science (Physics), Nagoya University Graduate School of Science, Nagoya, 464-8601, Japan

^c Department of Kinesiology and Outdoor Recreation, Southern Utah University, Cedar City, UT, 84720, USA

^d Molecular Hydrogen Institute, Enoch, UT, 84721, USA

^e Graduate School of Nutritional Sciences, Nagoya University of Arts and Sciences, Nisshin, 470-0196, Japan

ARTICLE INFO

Keywords:

Molecular hydrogen
Rieske iron-sulfur protein
Mitochondrial unfolded protein response
Hydrogenase

ABSTRACT

The mechanisms underlying the biomedical effects of molecular hydrogen (H_2) remain poorly understood and are often attributed to its selective reduction of hydroxyl radicals, based on the long-held notion that H_2 is biologically inert. We demonstrate that H_2 is biologically active, specifically targeting the Rieske iron-sulfur protein (RISP). We first observed that H_2 induces the mitochondrial unfolded protein response (UPR^{mt}) in cultured cells exposed to H_2 and in mouse liver after H_2 water administration. H_2 suppressed electron transport chain complex III activity in mouse liver homogenates to 78.5 % within 2 min. Given the evolutionary link with hydrogenases, we examined RISP as a potential target of H_2 . We found that H_2 promotes RISP degradation within 1 h in cultured cells by activating mitochondrial Lon peptidase 1 (LONP1). Loss of RISP and subsequent UPR^{mt} induction may explain the pleiotropic and paradoxical effects of H_2 . These findings identify RISP as a primary target of H_2 , demonstrating that H_2 is biologically active as a signaling molecule.

1. Introduction

The therapeutic potential of molecular hydrogen (H_2) dates back to 1793 and its reaction kinetics with hydroxyl radicals ($\cdot OH$) were characterized in the 1960s [1]. However, H_2 has long been regarded as biologically inert due to its small, neutral, and nonpolar nature, compounded by the absence of hydrogenase enzymes in humans. Unlike other signaling molecules such as the gasotransmitters, carbon monoxide (CO), hydrogen sulfide (H_2S), and nitric oxide (NO^\bullet), H_2 was presumed to lack the physicochemical properties necessary to interact with biological macromolecules. This presumption as a biologically inert gas justified its use as a safe, inert breathing gas for deep-sea diving since the 1940s [2] and relegated its role in physiology to that of a mere microbial byproduct [3].

Emerging evidence, however, suggests that increased endogenous H_2 production by the microbiome is associated with improved metabolic and cognitive health, reduced cardiovascular risk, and extended lifespan in centenarians [4]. However, no cogent mechanism has been provided

to explain these important observations.

A pivotal shift in the perception of H_2 occurred in 1975, when a *Science* publication reported that hyperbaric hydrogen, but not helium led to the marked regression of tumors in mice, attributed to its presumed ability to scavenge cytotoxic $\cdot OH$ radicals [5]. This mechanistic premise resurfaced more prominently in 2007 by a *Nature Medicine* study demonstrating that H_2 ameliorated brain damage in a rat stroke model [6]. Both studies relied on the radical scavenging mechanism. However, this concept is challenged by H_2 's slow second-order reaction rates relative to other more abundant nucleophilic biomolecules [7]. Nevertheless, research into H_2 has proliferated, with over 3000 publications, including 200 human studies highlighting its potential therapeutic effects [8]. Yet, the primary molecular target(s) and mechanisms of H_2 's activity have remained elusive, with much of the literature still framing H_2 as merely an antioxidant. Most recently, it was demonstrated that H_2 can bind to Fe-porphyrin and the hydrided Fe-porphyrin reduces hydroxyl radicals [9]. In addition, CO₂ bound to Fe-porphyrin is changed to CO by H_2 . However, the amounts of reduced hydroxyl radicals and the generated CO may be too low to exert efficient biological

* Corresponding author. Department of Kinesiology and Outdoor Recreation, Southern Utah University, Cedar City, UT, 84720, USA.

** Corresponding author. Division of Neurogenetics, Center for Neurological Diseases and Cancer, Nagoya University Graduate School of Medicine, Nagoya, 466-8550, Japan.

E-mail addresses: tylerlebaron@suu.edu (T.W. LeBaron), ohnok@med.nagoya-u.ac.jp (K. Ohno).

¹ These authors contributed equally to this work.

Abbreviations

ETC	Electron transport chain
LONP1	Mitochondrial Lon peptidase 1
RISP	Rieske iron-sulfur protein
ROS	Reactive oxygen species
UPR ^{mt}	Mitochondrial unfolded protein response

effects. Similarly, the concentrations of H₂ are too low and the dwell time of H₂ is too short *in cellulo* and *in vivo* [8,10] to account for the prolonged (i.e., hours to days) residual protective effects of H₂.

Given the limitations of the current proposed mechanisms, we hypothesized that H₂ might interact with an evolutionarily conserved hydrogenase-like protein harboring iron-sulfur [Fe-S] clusters. The Rieske iron-sulfur protein (RISP), encoded by *UQCRCFS1*, in Complex III of the mitochondrial electron transport chain (ETC) carries an [2Fe-2S] cluster and is a compelling candidate for interaction with H₂. RISP shuttles electrons from ubiquinol to cytochrome *c*₁ within the Q-cycle. Although RISP lacks a canonical H₂ activation or binding site, its conserved [2Fe-2S] cluster shares structural and evolutionary similarities with hydrogenase catalytic centers.

Mitochondrial dysfunction activates the mitochondrial unfolded protein response (UPR^{mt}), an adaptive pathway that maintains mitochondrial homeostasis through mitohormetic mechanisms [11]. Sobue et al. reported that H₂ induced UPR^{mt} in the mouse liver [12], and we previously showed that H₂ improved mitochondrial function in cells in which H₂ induced UPR^{mt} [13].

Here, we show that H₂ directly targets RISP, leading to its LONP1-mediated degradation, suppressing Complex III activity, and subsequently inducing UPR^{mt}. This targeted effect illuminates a previously unrecognized mechanism, redefining H₂ from a biologically inert molecule to a biologically active signaling molecule that modulates mitochondrial signaling pathways.

2. Materials and methods

2.1. Animal studies and ad libitum administration of H₂ water

All animal studies were approved by the Animal Care and Use Committee of the Nagoya University, and were conducted in accordance with relevant guidelines. Seven-week-old C57BL6/N mice were purchased from Japan SLC. H₂ water was freshly prepared every evening using Hydrogen Water 7.0 (Ecomo International), which was kindly provided by MiZ Co. Ltd. The H₂ concentrations in freshly prepared water were 2.5–3.5 mM. The H₂ concentration in the glass vessel that was inserted in the mouse cage decreased exponentially with a half-life of 1.09 h [35]. As mice drink water approximately every hour at night, mice were predicted to drink H₂ water with an average concentration of 1.7 mg/L [35]. At 7 weeks of age, mice started drinking H₂ water. After 4 weeks, mice were fasted for 17 h and were sacrificed under deep anesthesia with isoflurane. Whole liver tissue was collected and rapidly frozen in liquid nitrogen.

2.2. Cell culture and exposure to H₂ gas

We previously analyzed the effects of H₂ on AML12, A549, HCT116, HeLa, HepG2, HT1080, PC3, and SH-SY5Y cells, and found that the first five cells (AML12, A549, HCT116, HeLa, and PC3 cells) were more responsive to H₂ than the other cells [13]. As the four cell lines other than AML12 cells were cancer cells, we used AML12 cells that were derived from normal mouse hepatocytes. AML12 cells were purchased from ATCC. The cells were cultured in the DMEM/F-12 medium (Gibco) containing 10 % fetal bovine serum (FBS, Thermo Fisher Scientific),

dexamethasone (Sigma), and insulin-transferrin-sodium selenite (Sigma). Six- or 96-well culture plates were placed in a 560-ml closed plastic box that was humidified with water at the base of the box. The box was placed in an incubator (SLI-221, EYELA) and the air temperate inside the box was maintained at 37 °C. H₂ or N₂ gas (6 mL/min) was mixed with CO₂-added air (5 % CO₂ and 95 % air, 54 mL/min) to make 10 % H₂ or 10 % N₂ gas. As the air contains 78.1 % N₂, the N₂ concentration in the gas mixture labeled as 10 % N₂ gas is 76.8 %, but for simplicity it is referred to as 10 % N₂ gas in this communication. The mixed gas was introduced into the box via an afferent tube, and the box was equipped with an efferent tube to expel the gas outside the room. The concentration of H₂ in the medium was measured by equilibrating 1 mL of the medium with 100 mL of 100 % N₂ gas in an aluminum bag. Subsequently 1 mL of the equilibrated gas was analyzed via gas chromatography (EAGanalyzer GS-23). The cellular studies were performed in triplicate or quadruplicate on the same day, and the number of dishes is indicated in each figure legend. AML12 cells were treated with 2 mM N-acetylcysteine (NAC) for 18 h prior to exposure to 10 % H₂ for 1 h to examine whether reduction of reactive oxygen species (ROS) by H₂ mediates the reduction of RISP.

2.3. Measurements of mitochondrial ETC activities in mouse liver homogenates

ETC activities were measured as previously described [36]. Briefly, 5 μ L of the mouse liver homogenates or cell lysates were used for the reaction. The protein concentration of each sample was measured by the Pierce 660 nm protein assay reagent (Thermo Fisher Scientific). The activities of ETC complexes I, III, and IV were determined by the decrease in absorbance of NADH at 340 nm in 180 s, the increase in absorbance of reduced cytochrome *c* at 550 nm in 120 s, and the decrease in absorbance of reduced cytochrome *c* at 550 nm in 180 s, respectively, with NanoDrop 2000C (Thermo Fisher Scientific). We followed the incubation times in the previous report [36], and were not modulated in our assays. H₂ was dissolved in the reaction buffer using Hydrogen Water 7.0 (2.5–3.5 mM) immediately before the homogenates were added.

2.4. Inhibitors of ETC complex III

Antimycin A and myxothiazol were purchased from Sigma Aldrich. Variable concentrations of the chemicals were added to the culture medium for 12 h before harvesting cells.

2.5. Measurements of mitochondrial superoxide level and mitochondrial membrane potential

To evaluate the acute effects of H₂ on mitochondrial superoxide level and mitochondrial membrane potential in 10 and 30 min, H₂ was dissolved in the culture medium using Hydrogen Water 7.0 (2.5–3.5 mM) and was added to AML12 cells. To evaluate the delayed effects of H₂ over a period of 1–24 h, AML12 cells were cultured in an atmosphere of 10 % H₂ or 10 % N₂ gas as described above. After the cells were washed with PBS, the cells were incubated with either 5 μ L MitoSOX (M36008, Thermo Fisher Scientific) in Hank's balanced salt solution (HBSS, Gibco) or 100 nM tetramethylrhodamine (TMRM, T668, Thermo Fisher Scientific) in PBS at 37 °C for 30 min in an incubator. The cells were harvested using 0.25 % trypsin/0.1 % EDTA in PBS and centrifuged at 3000 \times g at 4 °C for 2 min. After washing with PBS, the signal intensities of MitoSOX and TMRM were quantified using a BD FACS Calibur (BD Science).

2.6. Measurement of *HSPD1* (*HSP60*) promoter activity by luciferase reporter assay

A 1333-bp segment of human *HSPD1* promoter (positions 197,499,187 to 197,500,519 according to GRCh38) was PCR-amplified

and cloned into the pGL4.10 luciferase reporter plasmid (Promega). AML12 cells were transfected with pGL4.10-HSPD1 and phRL-TK (Renilla luciferase plasmid, Promega) using Lipofectamine 2000 (Invitrogen) according to the manufacturer's protocols. Six hours post-transfection, cells were exposed to 10 % H₂ or 10 % N₂ gas for 18 h. Luciferase fluorescence was measured using the Dual Luciferase Reporter Assay System (Promega) with a PowerScan4 (DS Pharma Biomedical).

2.7. *Lonp1* knockdown and inhibition of LONP1 by CDDO-Me

siRNAs against mouse *Lonp1* were designed using the i-Score Designer [37]. The siRNA sequences were si783 (5'-GGUGGAGGUUGAGAAUGUA-3') and si1194 (5'-GGAGAAAGAUGAUAAAAGAU-3'). For *Lonp1* knockdown, AML12 cells were transfected with 150 pmol *Lonp1*-targeting siRNA (si783 or si1194) or control siRNA (AllStars Neg. Control siRNA, Qiagen) using Lipofectamine RNAiMax (Invitrogen) according to the manufacturer's protocols. At 48 h post-transfection, the cells were exposed to 10 % H₂ or 10 % N₂ gas for 1 or 12 h. To chemically inhibit LONP1, AML12 cells were treated with 0.1 or 1 μ M CDDO-Me (Sigma) and cultured in 10 % H₂ or 10 % N₂ gas for 1 h.

2.8. Preparation of cell lysates and Western blotting

Cells were harvested using PLC buffer containing 50 mM HEPES (pH 7.0), 150 mM NaCl, 10 % glycerol, 1 % TritonX-100, 1.5 mM MgCl₂, 1 mM EGTA, 100 mM NaF, 10 mM sodium pyrophosphate, 1 μ g/ μ L aprotinin, 1 μ g/ μ L leupeptin, 1 μ g/ μ L pepstatin A, 1 mM PMSF, 1 mM sodium orthovanadate, and the Phosphatase Inhibitor Cocktail (PhosSTOP, Roche). The lysates were mixed on a rotary shaker at 4 °C for 15 min and centrifuged at 17,900 $\times g$ at 4 °C for 15 min. The supernatants were boiled at 95 °C for 5 min in 2 \times Laemmli buffer. Samples were then loaded on a 10 % or 14 % SDS-polyacrylamide gel, and transferred to an Immobilon-P membrane (Millipore). Membranes were washed in Tris-buffered saline with 0.05 % Tween 20 (TBS-T), and blocked with 5 % skim milk in TBS-T at room temperature for 1 h. The membranes were incubated with primary antibodies (Supplementary Table S1) overnight at 4 °C. After washing with TBS-T, the membranes were incubated with secondary goat anti-mouse IgG (1: 5000, LNA931V/AG, GE Healthcare) or anti-rabbit IgG (1: 5000, LNA934V/AE, GE Healthcare) antibody conjugated to horseradish peroxidase (HRP) for 1 h at room temperature. The antibody-bound proteins were visualized using Amersham ECL Western blotting detection reagents (GE Healthcare), and the signal intensities were quantified using ImageQuant (GE Healthcare).

2.9. ATP quantification assay

AML12 cells were incubated in a 10 % N₂ gas atmosphere for 24 h before hydrogen exposure. The cells were then cultured in either 10 % H₂ or 10 % N₂ gas atmosphere for 1–24 h. The amount of ATP was quantified using Luminescent ATP Detection Assay Kit (ab113849, abcam).

2.10. Statistical analysis

All values were presented as the mean \pm SEM. For *in cellulo* studies, values were normalized to those of cells treated with 10 % N₂ gas, unless otherwise indicated. Statistical significance was assessed using Student's *t*-test, one-way ANOVA with Tukey's posthoc test, two-way ANOVA with Sidak's posthoc test, two-way ANOVA with Tukey's posthoc test, or the Jonckheere-Terpstra trend test using GraphPad Prism ver. 10.6.1 and IBM SPSS ver. 29.0.2.0. *P*-values less than 0.05 were considered statistically significant.

3. Results

3.1. H₂ modulates mitochondrial superoxide level and mitochondrial membrane potential

We examined the effects of H₂ on the mitochondrial superoxide production and the mitochondrial membrane potential in AML12 cells and found that both were decreased to 80.0 % and 78.1 %, respectively, in 10 min by exposure to 10 % H₂ gas (10 % H₂/4.5 % CO₂/85.5 % air) compared to control gas (10 % N₂/4.5 % CO₂/85.5 % air) (Fig. 1AB). However, the superoxide level and the membrane potential were increased to 116.6 % and 130.1 %, respectively, in 1 h, and to 137.2 % and 203.6 %, respectively, in 24 h. The early decrease and late increase of superoxide production and membrane potential suggest inhibition of the mitochondrial electron transport chain (ETC) and induction of mitohormesis.

3.2. H₂ induces UPR^{mt} in cultured cells and wild-type mouse liver

To determine the involvement of mitohormesis, we examined whether H₂ induces UPR^{mt} in the mouse liver-derived AML12 cells and in wild-type mouse liver. Compared to control gas, exposure of AML12 cells to 10 % H₂ gas for 6 h or longer increased the levels of UPR^{mt}-related proteins (PKR, *p*-eIF2 α , ATF5, and HSP60) (Fig. 2AB) and increased the promoter activity of *Hspd1* encoding HSP60 (Fig. 2C). Similarly, wild-type C57BL6/N mice that were administered H₂-rich water *ad libitum* for four weeks exhibited elevated levels of UPR^{mt}-related proteins (PKR, *p*-eIF2 α , ATF5, and HSP60) in the liver, although statistical significance was not observed in ATF5 or HSP60 (Fig. 2DE). We also examined the levels of mitochondria fission- and fusion-related proteins to evaluate the effects on mitochondrial dynamics. After 6 h of H₂ treatment, their expression levels remained unchanged in AML12 cells (Supplementary Fig. S1).

3.3. H₂ reduces ATP production and suppresses the enzymatic activity of ETC complex III

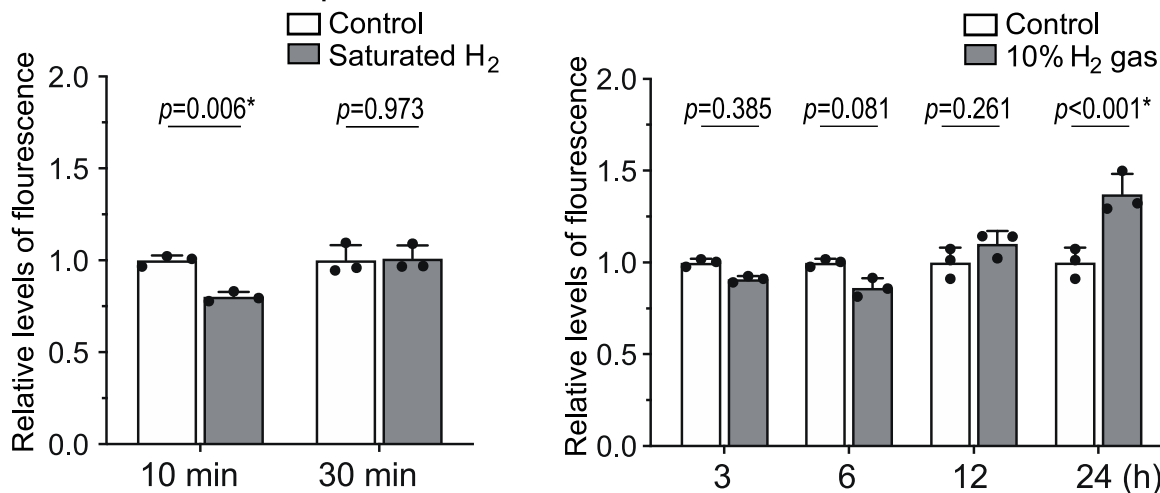
We next examined the effects of H₂ on the activities of mitochondrial ETC complexes I, III, and IV, which together constitute the major pathway to generate ATP from NADH. We found that exposing mitochondria isolated from wild-type C57BL6/N mouse liver to H₂-rich buffer for as little as 2 min suppressed the enzymatic activity of ETC complex III to 78.5 %; however, it did not reduce the activity of complexes I or IV (Fig. 3A). Thus, H₂ appeared to selectively suppress a critical subunit of ETC complex III.

3.4. H₂ modulates electron flow in complex III in the FeS-*c*₁ pathway

To dissect the effects of H₂ on ETC complex III, we added variable concentrations of complex III inhibitors, antimycin A and myxothiazol, to AML12 cells for 12 h, and evaluated the induction of UPR^{mt} by H₂. As shown in Fig. 3B, antimycin A blocks electron flow at the Q_i site (cytochrome b_H \rightarrow ubiquinone, Q) [14], whereas myxothiazol blocks electron flow at the Q_o site (ubiquinol, QH₂ \rightarrow cytochrome b_L) and thereby also electron flow into the FeS-*c*₁ pathway [15] resulting in a more complete blockage.

In control gas-treated AML12 cells, antimycin A induced UPR^{mt} in 12 h in a dose-dependent manner (Fig. 3CD), while myxothiazol failed to do so over the same time course (Fig. 3CE). Exposure to H₂ gas alone markedly induced UPR^{mt} (Fig. 3C-E). However, combining H₂ with antimycin A prevented UPR^{mt} induction (Fig. 3CD). This result mirrored the effects of myxothiazol, suggesting that H₂ may modulate electron transfer into the FeS-*c*₁ pathway. Partial inhibition of electron transfer by H₂ could disrupt electron flow and semiquinone radical formation, while the combination with antimycin A completely blocks electron transfer, thereby preventing semiquinone radical formation and the

A Mitochondrial superoxide level



B Membrane potential

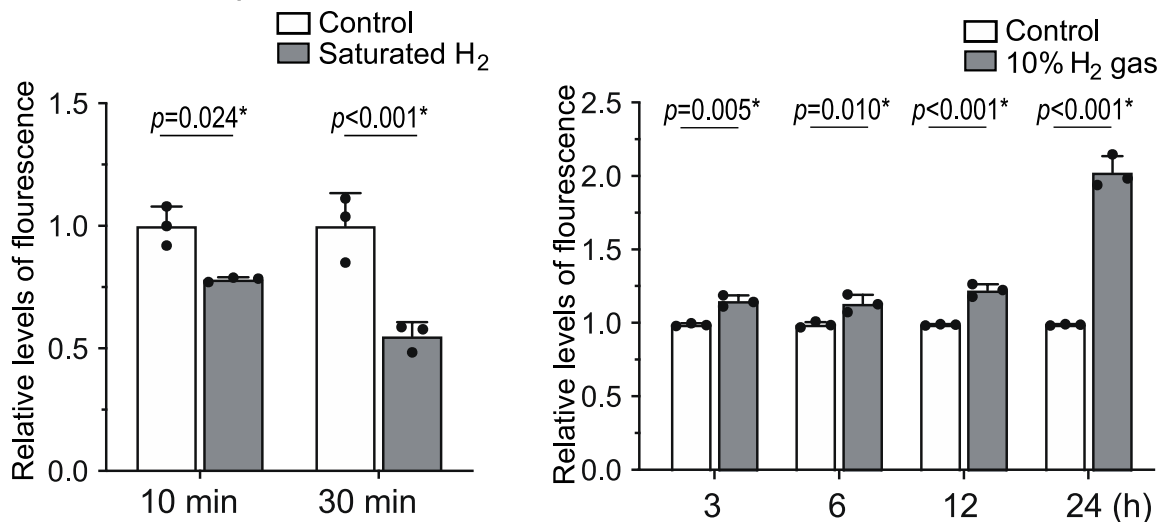


Fig. 1. H₂ initially decreased the mitochondrial ETC activities and subsequently upregulates them by inducing UPR^{mt}. AML12 cells incubated under 10 % H₂ or control gas for 10 min to 24 h were stained by MitoSOX for mitochondrial superoxide (A) and TMRM for mitochondrial membrane potential (B). For short-time exposures (left panels), the medium was saturated with H₂ in advance and was added to the cells. For long-term exposures (right panels), the culture plate was placed under 10 % H₂ or control gas. P-values by two-way ANOVA with Sidak's posthoc test ($n = 3$ culture dishes). Statistical significance is indicated by an asterisk.

induction of UPR^{mt}. Thus, the target of H₂ is likely to be in the FeS- c_1 pathway.

3.5. H₂ targets and decreases levels of the Rieske iron-sulfur protein (RISP)

Hydrogenases that directly react with H₂ as substrate contain an iron-sulfur cluster (Fe-S cluster) [16]. RISP encoded by *UQCRCFS1* is the only component in complex III containing an iron-sulfur cluster, and directly accepts electrons at the Q₀ site in the FeS- c_1 pathway (Fig. 3B). We thus examined the effects of H₂ on RISP and found that exposure to H₂ gas for 1 h decreased RISP to 73.3 % in AML12 cells (Fig. 4AB). To explore other potential hydrogen targets, we examined the amounts of representative mitochondrial oxidative phosphorylation complex proteins at 1 h of H₂ treatment, but no statistical difference was observed in these proteins (Supplementary Fig. S2). We also examined whether RISP degradation was mediated by reduced reactive oxygen species (ROS), such as hydroxyl radicals. To this end, AML12 cells were treated with 2 mM NAC for 18 h to reduce ROS and cultured with 10 % H₂ for 1 h. NAC

marginally reduced the amount of RISP without statistical significance. H₂ still reduced the amount of RISP even in the presence of NAC, confirming that lowering ROS is not a mediator of H₂-induced reduction of RISP (Fig. S3) (Supplementary Fig. S3). As NAC failed to cancel the effect of H₂, the decrease of RISP was unlikely to be mediated by H₂-mediated reduction of free radicals, if any. The RISP level resumed to baseline at 3 h and increased to 147.4 % at 6 h and 131.2 % at 24 h. In accordance with the decrease of RISP, H₂ gas decreased the ATP level to 85.1 % at 1 h, but resumed it to the basal level at 12 and 24 h (Fig. 4C). In contrast, the level of cytochrome c oxidase subunit I in complex IV that is encoded by *MT-CO1* on mitochondrial DNA remained unchanged up to 6 h but was increased to 155.4 % at 24 h (Fig. 4AB). As mitonuclear protein imbalance is one of the major causes inducing UPR^{mt} [17], transient reduction of RISP at 1 h likely initiated UPR^{mt}, which subsequently led to a compensatory increase in both RISP and MT-CO1 in 24 h. We also examined the effects of H₂ in other cell lines and found that H₂ treatment for 1 h decreased RISP in HT1080 and HeLa cells (Supplementary Fig. S4).

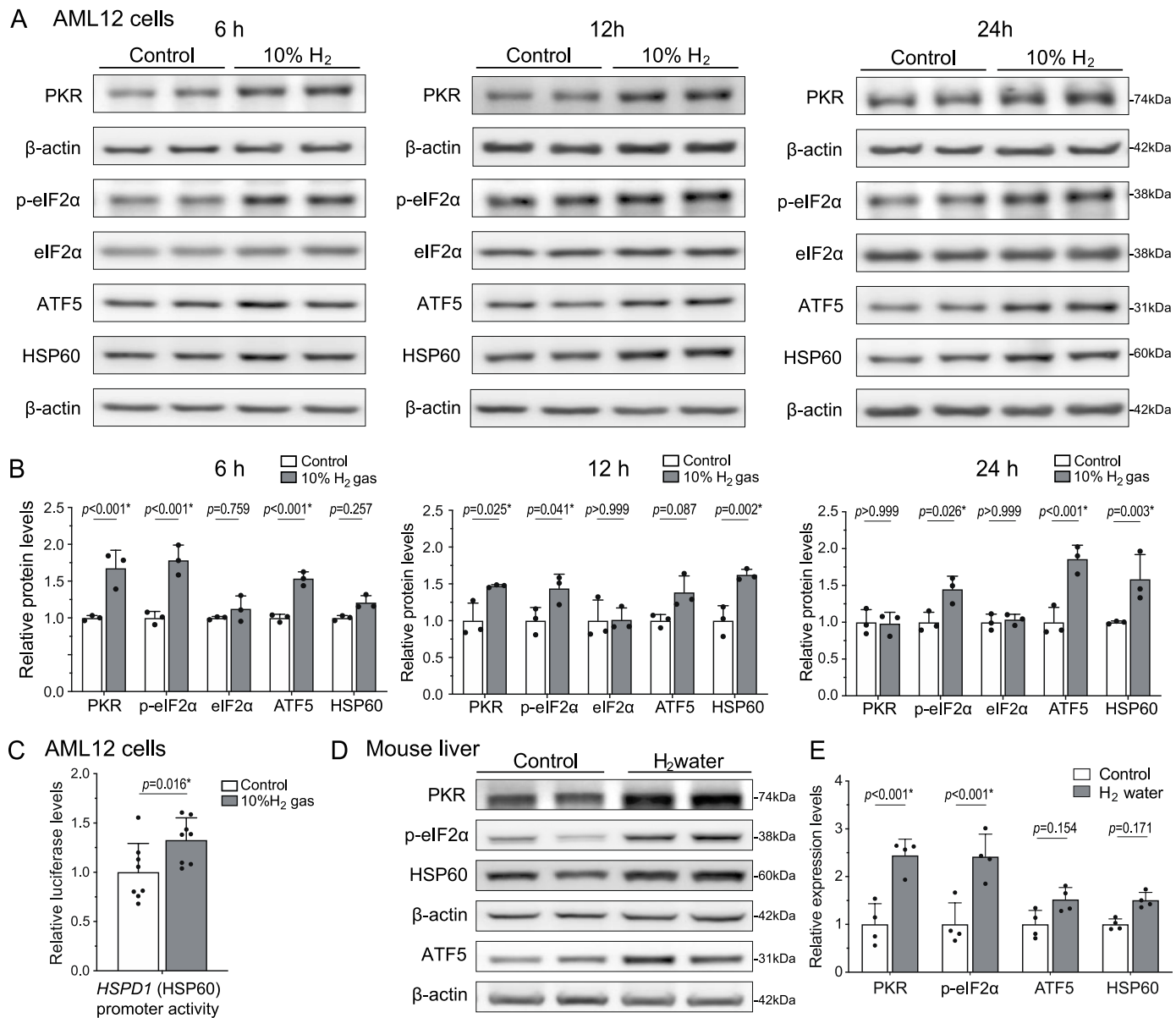


Fig. 2. H₂ induced UPR^{mt} in AML12 cells and the mouse liver. (A, B) AML12 cells were exposed to 10 % H₂ or control gas for 6, 12, and 24 h. Representative Western blotting (A) and quantification (B) of UPR^{mt}-related proteins (PKR, p-eIF2α, eIF2α, ATF5, and HSP60) in AML12 cells. P-values by two-way ANOVA with Sidak's posthoc test are indicated ($n = 3$ culture dishes each). * $P < 0.05$. (C) AML12 cells were exposed to 10 % H₂ or control gas for 18 h. The pGL4 luciferase activity of the human HSPD1 (HSP60) promoter was normalized for Renilla luciferase activity (pRL-TK) and also for the ratio in control cells. P-value by Student's *t*-test ($n = 8$ culture dishes each). * $P < 0.05$. (D, E) C57BL6/N mice were freely accessible to H₂-enriched water for 4 weeks. Representative Western blotting (D) and quantification (E) of UPR^{mt}-related proteins (PKR, p-eIF2α, ATF5, and HSP60) in the mouse liver. P-values by two-way ANOVA with Sidak's posthoc test are indicated ($n = 4$ mice each). Statistical significance is indicated by an asterisk.

3.6. Mitochondrial Lon peptidase 1, LONP1 mediates the H₂-induced degradation of RISP

Mitochondrial Lon peptidase 1 encoded by *LONP1* is a major mitochondrial protease that selectively degrades misfolded, unassembled, or damaged polypeptides in mitochondria, and plays a substantial role in the induction of UPR^{mt} [18]. We asked whether LONP1 was involved in the H₂-mediated degradation of RISP, and found that knockdown of LONP1 nullified the effects of H₂ on the decrease of RISP in 1 h (Fig. 5AB). Similarly, a LONP1 inhibitor, CDDO-Me, cancelled the effects of H₂ on the decrease of RISP in 1 h (Fig. 5CD). Thus, H₂ triggered LONP1-mediated degradation of RISP. In addition, LONP1 knockdown cancelled the increase of HSP60 expression by H₂ gas in 12 h (Fig. 5EF), indicating that a conformational change of RISP induced by H₂ is a key

to trigger LONP1 and UPR^{mt}. The selective degradation of RISP following LONP1 activation, which specifically targets misfolded/unfolded/damaged mitochondrial proteins, suggests that RISP is a primary target of H₂.

4. Discussion

Specific suppression of ETC complex III by H₂ and the presence of an iron-sulfur cluster in hydrogenases in evolution prompted us to examine the effects of H₂ on the only iron-sulfur cluster-bearing molecule in complex III, RISP. We indeed found that H₂ primarily targets RISP, and initiates its LONP1-mediated degradation. Notably, RISP is unique among mammalian iron-sulfur proteins in its coordination of the [2Fe-2S] cluster by two histidines, which elevate the cluster's redox

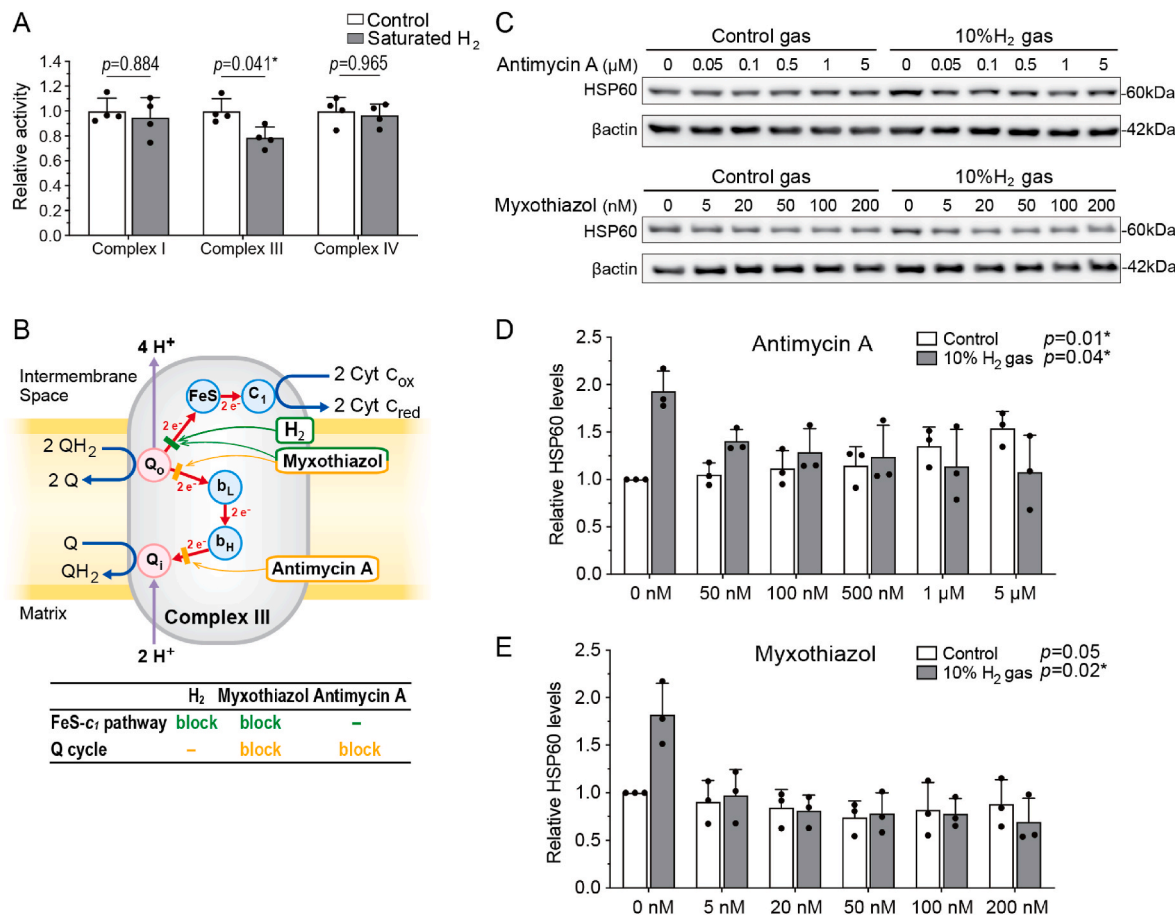


Fig. 3. H₂ decreased the ETC complex III activity by blocking the FeS-c₁ pathway. (A) Mitochondrial ETC complex activities of isolated mouse liver mitochondria exposed to H₂-saturated reaction buffer in 2–3 min. P-values by two-way ANOVA with Sidak's posthoc test are indicated (n = 4 mice each). *P < 0.05. (B) The Q cycle is blocked by both antimycin A and myxothiazol at different sites (yellow bars), whereas the FeS-c₁ pathway is blocked by myxothiazol and H₂ (green bar). Single blockade (antimycin A and H₂) preserves the responsiveness to UPR^{mt}, whereas double blockades (myxothiazol) abolish the responsiveness. Q, ubiquinone. FeS, RISP. (C, D, E) Representative Western blotting (C) and quantification of HSP60 (D, E) in AML12 cells exposed to 10 % H₂ or control gas in the presence of complex III inhibitors, antimycin A (C, D) or myxothiazol (C, E), for 12 h. P-values by Jonckheere-Terpstra trend test are indicated (n = 3 culture dishes each). The Jonckheere-Terpstra trend test examines whether the change of values is monophasic or not, and gives a single p-value for each condition. Statistical significance is indicated by an asterisk.

potential compared to the cysteine-only coordination seen in other iron-sulfur proteins [19]. This unique configuration may underlie RISP's favorable interaction with H₂, in contrast to other cysteine-coordinated iron-sulfur-bearing proteins that appear unresponsive to H₂ [20].

The amount of RISP should be determined by a balance between LONP1-mediated degradation and its subsequent compensatory UPR^{mt}-mediated induction. In the presence of H₂, LONP1 continues to degrade RISP, initiating a transient mitonuclear protein imbalance that triggers UPR^{mt}. This compensatory response upregulates RISP synthesis, leading to a recovery and eventual overshoot of RISP levels at later time points, as observed at 6 and 24 h (Fig. 4B). We previously showed that ingestion of H₂ water or intermittent inhalation of H₂ gas, but not continuous inhalation of H₂ gas, ameliorated a rat model of Parkinson's disease [21]. These results may be accounted for by the discontinuation of RISP degradation by intermittent H₂ inhalation or drinking H₂ water. This suggests that intermittent exposure to H₂ is sufficient to optimize the balance between stress induction and adaptive recovery, a hallmark of hormesis.

We found that the induction of UPR^{mt} was associated with a biphasic modulation of mitochondrial superoxide production, membrane potential, ATP levels, and the enzymatic activity of ETC Complex III, suggesting a tightly regulated hormetic response. The initial suppression of superoxide and membrane potential within 10 min of H₂ exposure (Fig. 1AB) likely reflects transient inhibition of electron flow through

Complex III, as evidenced by the reduction of its enzymatic activity to 78.5 % observed in isolated mitochondria (Fig. 3A). This disruption correlated with a decrease in ATP levels to 85.1 % at 1 h (Fig. 4C), indicative of reduced mitochondrial activity. However, over the subsequent hours, superoxide production and membrane potential increased significantly (Fig. 1AB), corresponding to the restoration of ATP levels to baseline by 12 and 24 h (Fig. 4C). This compensatory response likely reflects an adaptive enhancement of mitochondrial function driven by mitochondrial hormesis. While the magnitude of UPR^{mt} induction in AML12 cells by H₂ was less pronounced compared to studies using chemical stress inducers or genetic engineering to provoke mitonuclear imbalance [11], it is important to note that these experimental conditions exceed physiological feasibility and relevance. In contrast, even high doses/concentrations of H₂ can be readily applied to humans without adverse effects [22].

The biphasic mitochondrial dynamics observed in this study reconcile seemingly contradictory findings in previous reports on markers of reactive oxygen species (ROS) and inflammation. Similar to other small gaseous signaling molecules (NO[•], CO, H₂S) [23], H₂ has been shown to paradoxically increase or decrease various molecules, pathways, and indicators. These include malondialdehyde [24], derivatives of reactive oxygen species [25], superoxide levels [26], 8-hydroxy deoxyguanine [27], Nrf2 [28], NF-κB [28,29], heat shock proteins [30], ATP levels [6, 26], mitochondrial membrane potential [31], and ETC complex activity

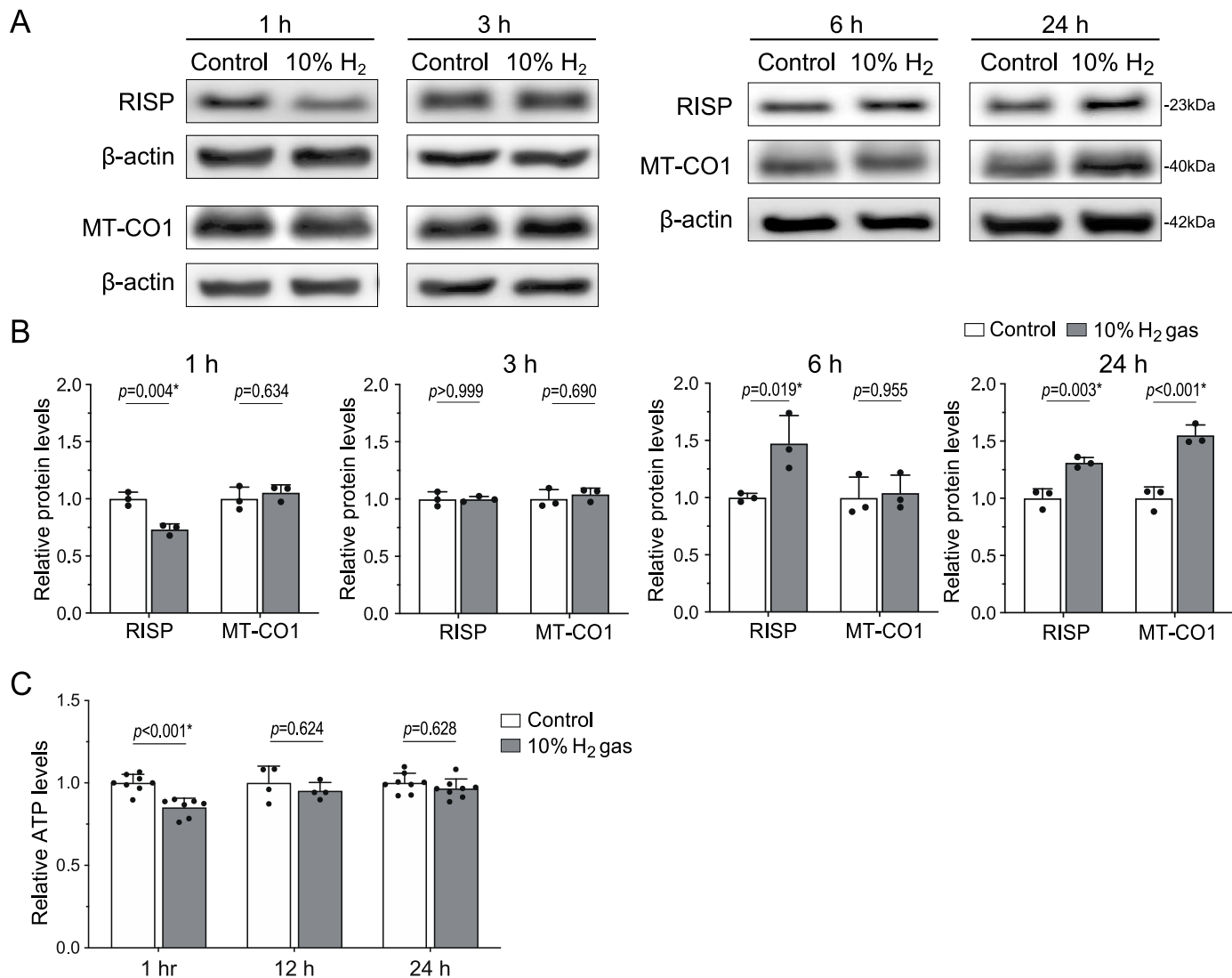


Fig. 4. H₂ decreased RISP in 1 h and increased it at 6 h and 24 h in AML12 cells. (A, B) Representative Western blotting (A) and quantification (B) of nuclear DNA-encoded RISP and mitochondrial DNA-encoded MT-CO1 in AML12 cells cultured under 10 % H₂ or control gas for 1, 3, 6, and 24 h. *P*-values by two-way ANOVA with Sidak's posthoc test are indicated (*n* = 3 culture dishes). **P* < 0.05. (C) ATP levels of AML12 cells cultured under 10 % H₂ or control gas for 1, 12, and 24 h. *P*-values by two-way repeated measures ANOVA with Sidak's posthoc test (*n* = 7, 4, and 8 culture dishes each at 1, 12, and 24 h, respectively). Statistical significance is indicated by an asterisk.

[32], and mitophagy [33], while simultaneously providing therapeutic effects that promote cellular survival under stress conditions. Early mechanistic studies proposed that H₂ exerted its effects not as a biologically active molecule, but solely through its chemical property of reacting with hydroxyl radicals [6,9]. Thus, these studies fail to account for H₂'s temporally dynamic and seemingly paradoxical effects on redox and inflammatory pathways. In contrast, our findings reveal that H₂ is a biologically active agent, mediating its biphasic response through the selective modulation of Complex III, altering electron transport to trigger mitochondrial signaling and adaptive stress pathways, such as UPR^{mt}.

Mitochondria are descendants of ancient hydrogenase that relied on H₂ for their energy systems and redox regulation long before oxygen dominated Earth's atmosphere [34]. In this study, we demonstrate that molecular hydrogen, a gas integral to early life forms, specifically targets RISP within mitochondrial ETC Complex III. This hormetic interaction links two primordial elements, mitochondria and hydrogen, and redefines H₂ from a biologically inert molecule to a biologically active signaling molecule. Given the growing body of clinical research on H₂, elucidating its precise mechanism of action provides critical insights that can guide the design and interpretation of future clinical studies to evaluate its effectiveness and optimize its therapeutic potential.

that can guide the design and interpretation of clinical trial protocols, optimizing its therapeutic potential.

Our study has the following limitation. Although we showed that H₂ induced LONP1-mediated degradation of RISP, we did not examine the exact conformational changes in RISP induced by H₂ or how LONP1 recognized H₂-exposed RISP as a target for degradation.

5. Conclusion

We showed that H₂ primarily targets RISP in mitochondrial ETC complex III. This targeting leads to (i) LONP1-mediated degradation of RISP, (ii) initial suppression of mitochondrial ETC activity, followed by (iii) activation of mitochondrial ETC activity via induction of UPR^{mt} by mitonuclear protein imbalance and increased reactive oxygen species. The elucidated mechanism readily accounts for the temporally diverse and ostensibly paradoxical effects of H₂ on redox and inflammatory markers. Given the growing body of clinical research on H₂, elucidating its precise mechanism of action provides critical insights that can guide the design and interpretation of future clinical studies to evaluate its effectiveness and optimize its therapeutic potential.

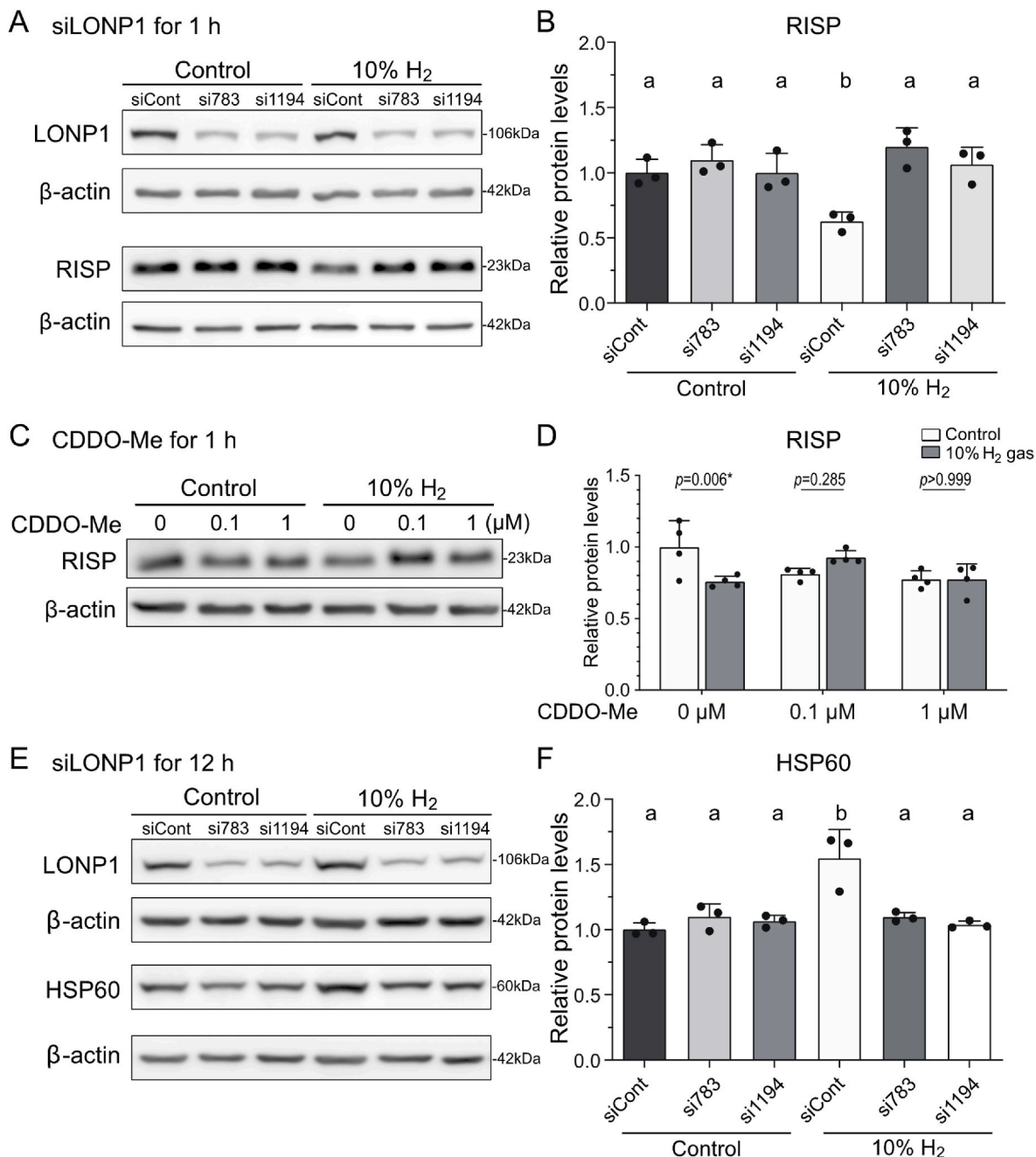


Fig. 5. Inhibition of LONP1 by knockdown or a specific inhibitor cancelled the reduction of RISP by H₂ in AML12 cells. Representative Western blotting (A, E) and quantification (B, D, F) of RISP (A, B, C, D) and HSP60 (E, F) in AML12 cells cultured under 10 % H₂ or control gas, while LONP1 was knocked down by si783 or si1194 (A, B, E, F) or inhibited by CDDO-Me (C, S) ($n = 3, 4$, and 3 culture dishes for B, D, and F, respectively). (B, F) $P < 0.05$ by one-way ANOVA with Tukey's posthoc test is indicated by 'a' and 'b'. (D) P -values by two-way ANOVA with Sidak's posthoc test (asterisk indicates statistical significance).

CRediT authorship contribution statement

Shuto Negishi: Investigation, Writing – original draft, Methodology. **Mikako Ito:** Conceptualization, Formal analysis, Project administration, Writing – original draft, Investigation, Methodology, Funding acquisition. **Tomoya Hasegawa:** Investigation. **Hikaru Otake:** Investigation. **Bisei Ohkawara:** Methodology, Project administration. **Akio Masuda:** Methodology, Project administration. **Hiroyuki Mino:** Methodology, Supervision. **Tyler W. LeBaron:** Conceptualization, Supervision, Writing – review & editing. **Kinji Ohno:** Conceptualization, Supervision, Writing – review & editing, Funding acquisition.

Data and materials availability

The data that support the findings of this study are available from the corresponding authors upon reasonable request.

Funding

This work was supported by Grants-in-Aid from the Japan Agency for Medical Research and Development (JP23ek0109678); the Japan Society for the Promotion of Science (JP23H02794, JP23K18273, JP21H02476, JP22K19269, and JP23K06412); the Ministry of Health, Labour and Welfare of Japan (23FC1014); and the National Center of Neurology and Psychiatry (5-6).

Declaration of competing interest

The authors declare no conflict of interest.

Acknowledgments

We would like to acknowledge MiZ Co. Ltd. for providing us with Hydrogen Water 7.0 (Ecomo International).

Appendix A. Supplementary data

Supplementary data to this article can be found online at <https://doi.org/10.1016/j.redox.2025.103952>.

References

- [1] T.W. LeBaron, K. Ohno, J.T. Hancock, *Oxygen* 3 (1) (2023) 143, <https://doi.org/10.3390/oxygen3010011>.
- [2] H. Bjurstedt, G. Severin, *Mil. Surg.* 103 (2) (1948) 107.
- [3] A. Strocchi, M.D. Levitt, *Gastroenterology* 102 (4 Pt 1) (1992) 1424.
- [4] Y. Ichikawa, H. Yamamoto, S.I. Hirano, B. Sato, Y. Takefuji, F. Satoh, *Med. Gas Res.* 13 (3) (2023) 108, <https://doi.org/10.4103/2045-9912.344977>.
- [5] M. Dole, F.R. Wilson, W.P. Fife, *Science* 190 (4210) (1975) 152, <https://doi.org/10.1126/science.1166304>.
- [6] I. Ohsawa, M. Ishikawa, K. Takahashi, M. Watanabe, K. Nishimaki, K. Yamagata, K. Katsura, Y. Katayama, S. Asoh, S. Ohta, *Nat. Med.* 13 (6) (2007) 688, <https://doi.org/10.1038/nm1577>.
- [7] K.C. Wood, M.T. Gladwin, *Nat. Med.* 13 (6) (2007) 673, <https://doi.org/10.1038/nm0607-673>.
- [8] T.W. LeBaron, R. Sharpe, K. Ohno, *Int. J. Mol. Sci.* 23 (23) (2022) 14750, <https://doi.org/10.3390/ijms232314750>.
- [9] Z. Jin, P. Zhao, W. Gong, W. Ding, Q. He, *Nano Res.* 16 (2) (2022) 2020, <https://doi.org/10.1007/s12274-022-4860-y>.
- [10] T.W. LeBaron, R. Sharpe, K. Ohno, *Int. J. Mol. Sci.* 23 (23) (2022) 14508, <https://doi.org/10.3390/ijms232314508>.
- [11] a) Q. Zhao, J. Wang, I.V. Levichkin, S. Stasinopoulos, M.T. Ryan, N.J. Hoogenraad, *EMBO J.* 21 (17) (2002) 4411, <https://doi.org/10.1093/emboj/cdf445>; b) C.J. Fiorese, A.M. Schulz, Y.F. Lin, N. Rosin, M.W. Pellegrino, C.M. Haynes, *Curr. Biol.* 26 (15) (2016) 2037, <https://doi.org/10.1016/j.cub.2016.06.002>; c) E. Fessler, E.M. Eckl, S. Schmitt, I.A. Mancilla, M.F. Meyer-Bender, M. Hanf, J. Philippou-Massier, S. Krebs, H. Zischka, L.T. Jae, *Nature* 579 (7799) (2020) 433, <https://doi.org/10.1038/s41586-020-2076-4>; d) X. Guo, G. Aviles, Y. Liu, R. Tian, B.A. Unger, Y.T. Lin, A.P. Wiita, K. Xu, M. A. Correia, M. Kampmann, *Nature* 579 (7799) (2020) 427, <https://doi.org/10.1038/s41586-020-2078-2>.
- [12] S. Sobue, C. Inoue, F. Hori, S. Qiao, T. Murate, M. Ichihara, *Biochem. Biophys. Res. Commun.* 493 (1) (2017) 318, <https://doi.org/10.1016/j.bbrc.2017.09.024>.
- [13] T. Hasegawa, M. Ito, S. Hasegawa, M. Teranishi, K. Takeda, S. Negishi, H. Nishiwaki, J.I. Takeda, T.W. LeBaron, K. Ohno, *Int. J. Mol. Sci.* 23 (5) (2022) 2888, <https://doi.org/10.3390/ijms23052888>.
- [14] a) P. Benit, S. Lebon, P. Rustin, *Biochim. Biophys. Acta* 1793 (1) (2009) 181, <https://doi.org/10.1016/j.bbamer.2008.06.004>; b) M. Labs, T. Ruhle, D. Leister, *Photosynth. Res.* 129 (3) (2016) 231, <https://doi.org/10.1007/s11120-016-0217-2>.
- [15] A.R. Crofts, B. Barquera, R.B. Gennis, R. Kuras, M. Guergova-Kuras, E.A. Berry, *Biochemistry* 38 (48) (1999) 15807, <https://doi.org/10.1021/bi990962m>.
- [16] a) M.W. Adams, E. Eccleston, J.B. Howard, *Proc. Natl. Acad. Sci. USA* 86 (13) (1989) 4932, <https://doi.org/10.1073/pnas.86.13.4932>; b) A.J. Pierik, W.R. Hagen, J.S. Redeker, R.B. Wolbert, M. Boersma, M.
- [17] F. Verhagen, H.J. Grande, C. Veeger, P.H. Mutsaers, R.H. Sands, et al., *Eur. J. Biochem.* 209 (1) (1992) 63, <https://doi.org/10.1111/j.1432-1033.1992.tb17261.x>.
- [18] L. Mouchiroud, R.H. Houtkooper, N. Moullan, E. Katsyuba, D. Ryu, C. Canto, A. Mottis, Y.S. Jo, M. Viswanathan, K. Schoonjans, L. Guarente, J. Auwerx, *Cell* 154 (2) (2013) 430, <https://doi.org/10.1016/j.cell.2013.06.016>.
- [19] a) T.A. Link, W.R. Hagen, A.J. Pierik, C. Assmann, G. von Jagow, *Eur. J. Biochem.* 208 (3) (1992) 685, <https://doi.org/10.1111/j.1432-1033.1992.tb17235.x>; b) S. Iwata, M. Saynovits, T.A. Link, H. Michel, *Structure* 4 (5) (1996) 567, [https://doi.org/10.1016/s0969-2126\(96\)00062-7](https://doi.org/10.1016/s0969-2126(96)00062-7).
- [20] J. Penders, R. Kissner, W.H. Koppenol, *Free Radic. Biol. Med.* 75 (2014) 191, <https://doi.org/10.1016/j.freeradbiomed.2014.07.025>.
- [21] M. Ito, M. Hirayama, K. Yamai, S. Goto, M. Ito, M. Ichihara, K. Ohno, *Med. Gas Res.* 2 (1) (2012) 15, <https://doi.org/10.1186/2045-9912-2-15>.
- [22] a) T. Tamura, H. Narumiya, K. Homma, M. Suzuki, G. Efficacy of Inhaled Hydrogen on Neurologic Outcome Following Brain Ischemia During PostCardiac Arrest Care Study, *Crit. Care Med.* 52 (10) (2024) 1567, <https://doi.org/10.1097/CCM.0000000000006395>; b) M. Chair, H. AlAani, S. Lafci Fahrioglu, C. Ben Hamda, U. Fahrioglu, T. Degheidy, *Free Radic. Biol. Med.* 222 (2024) 601, <https://doi.org/10.1016/j.freeradbiomed.2024.07.010>.
- [23] R.F. Coburn, *Front. Pharmacol.* 12 (2021) 830241, <https://doi.org/10.3389/fphar.2021.830241>.
- [24] a) G.A. Matchett, N. Fathali, Y. Hasegawa, V. Jadhav, R.P. Ostrowski, R.D. Martin, I.R. Dorotta, X. Sun, J.H. Zhang, *Brain Res.* 1259 (2009) 90, <https://doi.org/10.1016/j.brainres.2008.12.066>; b) J.M. Eckermann, W. Chen, V. Jadhav, F.P. Hsu, A.R. Colahan, J. Tang, J. H. Zhang, *Med. Gas Res.* 1 (1) (2011) 7, <https://doi.org/10.1186/2045-9912-1-7>.
- [25] K. Aoki, A. Nakao, T. Adachi, Y. Matsui, S. Miyakawa, *Med. Gas Res.* 2 (1) (2012) 12, <https://doi.org/10.1186/2045-9912-2-12>.
- [26] Y. Murakami, M. Ito, I. Ohsawa, *PLoS One* 12 (5) (2017) e0176992, <https://doi.org/10.1371/journal.pone.0176992>.
- [27] M. Hirayama, M. Ito, T. Minato, A. Yoritaka, T.W. LeBaron, K. Ohno, *Med. Gas Res.* 8 (4) (2018) 144, <https://doi.org/10.4103/2045-9912.248264>.
- [28] C.M. Zheng, Y.C. Hou, M.T. Liao, K.W. Tsai, W.C. Hu, C.C. Yeh, K.C. Lu, *Biomed. Pharmacother.* 176 (2024) 116802, <https://doi.org/10.1016/j.biopha.2024.116802>.
- [29] S. Sobue, K. Yamai, M. Ito, K. Ohno, M. Ito, T. Iwamoto, S. Qiao, T. Ohkuwa, M. Ichihara, *Mol. Cell. Biochem.* 403 (1–2) (2015) 231, <https://doi.org/10.1007/s11010-015-2353-y>.
- [30] a) H. Nishiwaki, M. Ito, S. Negishi, S. Sobue, M. Ichihara, K. Ohno, *Free Radic. Res.* 52 (4) (2018) 434, <https://doi.org/10.1080/10715762.2018.1439166>; b) T.W. LeBaron, I. Laher, B. Kura, J. Slezak, *Can. J. Physiol. Pharmacol.* 97 (9) (2019) 797, <https://doi.org/10.1139/cjpp-2019-0067>.
- [31] Y.S. Yu, H. Zheng, *Mol. Cell. Biochem.* 365 (1–2) (2012) 233, <https://doi.org/10.1007/s11010-012-1264-4>.
- [32] K. Noda, N. Shigemura, Y. Tanaka, J. Bhama, J. D'Cunha, H. Kobayashi, J. Luketich, C.A. Bermudez, *Transplantation* 98 (5) (2014) 499, <https://doi.org/10.1097/TP.0000000000000254>.
- [33] L. Yao, H. Chen, Q. Wu, K. Xie, *Int. J. Mol. Med.* 44 (3) (2019) 1048, <https://doi.org/10.3892/ijmm.2019.4264>.
- [34] W. Martin, M. Muller, *Nature* 392 (6671) (1998) 37, <https://doi.org/10.1038/32096>.
- [35] S. Hasegawa, M. Ito, M. Fukami, M. Hashimoto, M. Hirayama, K. Ohno, *Redox Rep.* 22 (1) (2017) 26, <https://doi.org/10.1080/13510002.2015.1135580>.
- [36] T. Toda, M. Ito, J.I. Takeda, A. Masuda, H. Mino, N. Hattori, K. Mohri, K. Ohno, *Commun. Biol.* 5 (1) (2022) 453, <https://doi.org/10.1038/s42003-022-03389-7>.
- [37] M. Ichihara, Y. Murakumo, A. Masuda, T. Matsuura, N. Asai, M. Jijiwa, M. Ishida, J. Shinmi, H. Yatsuya, S. Qiao, M. Takahashi, K. Ohno, *Nucleic Acids Res.* 35 (18) (2007) e123, <https://doi.org/10.1093/nar/gkm699>.